ACS APPLIED MATERIALS & INTERFACES

Research Article

www.acsami.org

A Turn-on Fluorescent Nanoprobe for Selective Determination of Selenium(IV)

Song Liang, Jiao Chen, David T. Pierce, and Julia Xiaojun Zhao*

Department of Chemistry, University of North Dakota, Grand Forks, North Dakota 58202, United States

ABSTRACT: A turn-on fluorescent nanoprobe was developed for selective determination of selenium(IV). A trace amount of selenium, as an essential nutrient, plays an important role in human health. It has been proven that a selenium deficiency will result in serious health problems. The developed nanoprobe is capable of in situ detection of selenium with target-induced signaling, and no separation step is needed. The nanoprobe consists of a silica nanoparticle core and a coating layer containing selenium(IV)-induced fluorescent molecules, 3,3′-diaminobenzidine (DAB). The nanoprobes have no fluorescence signals if they are not exposed to selenium(IV). However, the nanoprobes will be "turned on", with fluorescence, when they bind to the targets of selenium(IV). With this strategy, the selenium(IV) are first collected and enriched on a small domain of the nanoprobes. Then, with an excitation at 420 nm, the nanoprobes emit fluorescence signals at 530 nm. The fluorescence intensity is proportional to the selenium concentration. A fluorescence microscope was used to monitor the process of enriching and collecting of the selenium(IV) by the nanoprobes. The optimal conditions for the determination of selenium(IV) using the nanoprobe were investigated including pH, solvent, and linear range. The interference from common metal ions was studied as well. This study is expected to shed light on how to design turn-on fluorescent nanoprobes for in situ monitoring of a wide variety of targets in biological processes.

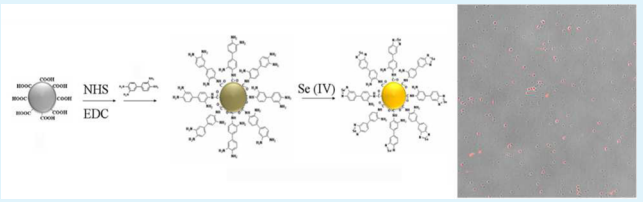

KEYWORDS: *fluorescence, nanoprobe, selenium, turn-on, target-induced signal*

1. INTRODUCTION

A trace amount of selenium, as an essential nutrient, plays an important role in human health.[1−3] Usually, in human bodies selenium presents in the form of selenoproteins that are involved in a multitude of cellular proliferation processes.[2] It has been proven that a selenium deficiency will result in serious health problems, such as a decrease in immune and thyroid function, high risk of some cancers[2−4] including breast cancer[4] and prostate cancer,[5] and Keshan and Kaschin−Beck diseases. Recently, research results have also demonstrated preventive effects of selenium on cancers.

Although selenium is an essential element, it will become toxic if its concentration exceeds a safe limit. In general, selenium is required by the human body in the range of 0.10−0.30 μg/kg. A higher concentration of selenium, such as 2.00 to 10.00 μg/kg, produces chronic toxic symptoms including liver carcinoma, cirrhosis, loss of teeth, and paralysis. In the United States, the recommended dietary allowance of selenium for adults is 55.00 μg/day.[3]

Due to this biological significance, the monitoring of selenium concentration is very important. Currently, several methods have been used to determine trace amounts of selenium, such as fluorometry,[6,7] atomic spectrometry,[8−12] mass spectrometry,[13] and stripping voltammetry.[14,15] Some of these methods can detect selenium with very high sensitivities. However, in situ detection is a challenge since these methods all are based on off-line detections. In situ detection of selenium is very important for some cellular and food samples. Thus, the development of in situ methods for selective determination of selenium is needed.

Fluorescent nanomaterials are revolutionary materials for sensitive and selective determination of trace amounts of targets.[16−18] So far, several types of fluorescent nanomaterials have been developed, such as quantum dots,[19−21] fluorescent polymer nanoparticles,[22,23] and fluorescent silica nanoparticles.[24−28] Fluorescent nanoparticles have been widely used in biomedical applications as substitutes for molecular fluorophores. Compared to the traditional fluorescent molecules, these fluorescent nanomaterials demonstrate excellent photostabilities and high sensitivities for signaling trace amounts of targets. Among the above fluorescent nanomaterials, silica-based fluorescent nanoparticles have been studied with great interest. Fluorescent silica nanoparticles are synthesized by encapsulating dye molecules inside the silica matrix or attaching dye molecules on their surfaces. Collecting thousands of dye molecules, a fluorescent silica nanoparticle is much brighter than a single fluorophore. It has been proven that fluorescent silica nanoparticles are excellent labeling reagents for the sensitive detection of several biological species.[29−31]

However, the fluorescence of these nanomaterials is intrinsic, and their fluorescence intensity does not change accordingly as the targets are bound to the nanomaterials. Thus, these

Received: March 19, 2013
Accepted: May 15, 2013
Published: May 15, 2013

   dx.doi.org/10.1021/am401015d | ACS Appl. Mater. Interfaces 2013, 5, 5165−5173

fluorescent nanomaterials can only serve as a fluorescent labeling reagent, but not an in situ probe for target binding. Moreover, because the fluorescence is permanent and not "turned on" in the presence of analytes, a separation procedure is needed to remove unbound fluorescent nanomaterials from the analyte matrix. Complete removal of unbound fluorescent nanomaterials from the detection system remains as a major impediment for further reduction in background signals.

In this work we have developed a new type of fluorescent nanomaterials, a turn-on fluorescent nanoprobe, with an ability of target-induced signaling for in situ detection of selenium, and no separation step is needed. This nanoprobe was designed by immobilizing of a large number of 3,3′-diaminobenzidine (DAB) molecules on the surface of a carboxyl group modified silica nanoparticle. DAB molecules alone have little fluorescence signal since DAB does not have large conjugated planar π bonds. Upon capturing of Se(IV), a fluorescent complex of DAB−Se, 3′,4′-diaminophenylpiazselenol, is formed.[6] Due to a large number of DAB on a single nanoparticle, the nanoprobe can be "turned on" with strong fluorescence when they bind to the target of selenium(IV). The fluorescence intensity is variable based on the amount of selenium bound to the nanoprobe; thus, the in situ monitoring of selenium can be achieved using this nanoprobe. Meanwhile, the nanoprobe showed no or low fluorescence signal in the absence of target selenium. Thus, no separation process is needed to reduce the fluorescence background signals. This study is expected to shed light on how to design turn-on fluorescent nanoprobes for in situ monitoring of a wide variety of targets in biological processes.

2. EXPERIMENTAL SECTION

2.1. Chemicals and Apparatus. Triton X-100 (polyethylene glycol *p*-(1,1,3,3-tetramethylbutyl)phenyl ether), tetraethyl orthosilicate (TEOS, 99.999%), *N*-((trimethyloxy)silylpropyl)ethylenediamine triacetic acid trisodium salt (TOETAT, 45% in water); 2-(*N*-morpholino)-ethanesulfonic acid (MES); 1-ethyl-3-(3-dimethylaminopropyl) carbodiimide hydrochloride (EDC); *N*-hydroxysuccinimide (NHS); 1,000 ppm Se(IV) standard solutions (in HNO_3); and 3,3′-diaminobenzidine (DAB) were purchased from Aldrich Chemical Co. Inc. Toluene, isopropanol, cyclohexane, *n*-hexanol, potassium phosphate dibasic, sodium phosphate monobasic, sodium chloride, and aqueous ammonia solution (NH_4OH, 29%) were purchased from Fisher Scientific Co. Ultrapurified water (18.3 MΩ·cm) used in the all experiments was obtained from a Milli-Q Millipore system.

A Shimadzu UV-250PC UV−vis spectrophotometer was used to measure the absorbance of sample solution. A Jobin Yvon Horiba Flourolog-3 spectrofluorometer was employed to obtain the fluorescence emission and excitation spectra. A Hitachi 4700 field emission scanning electron microscope (SEM) was used to take SEM images. An Olympus IX71 fluorescence microscope with a C9100 EM-CCD digital camera (Hamamatsu) was used to obtain bright field and fluorescence images. An Eppendorf 5804 centrifuge was used for separation of the nanoparticles from supernatant. A PQ ExCell ICP-AES was used for the elemental analysis with the experimental conditions of auxiliary flow rate of 0.79 L/min and nebulizer pressure of 2.56 bar.

2.2. Synthesis of Carboxyl Group Modified Silica Nanoparticles. A reverse microemulsion method was employed to synthesize COOH-modified silica nanoparticles.[32] An aliquot was prepared by mixing together 7.5 mL of cyclohexane, 1.8 mL of *n*-hexanol, and 1.77 mL of Triton X-100 (surfactant). To form an isotropic and thermodynamically stable microemulsion, 480 μL of water was added to the mixture. In the presence of 50 μL of TEOS, a polymerization reaction was initiated by adding a small amount of 29% NH_4OH (60 μL). After continuous stirring for 24 h, silica nanoparticles were formed in the microemulsion. Then, a postcoating process was carried out by adding 50 μL of TEOS and 50 μL of 45% TOETAT to the microemulsion. The mixture was stirred continuously for another 24 h. Finally, an outer layer containing carboxyl groups was formed on the silica nanoparticle surface. Then, acetone was added to break the microemulsion to release the nanoparticles. To remove the surfactant from the nanoparticles, the products were washed with acetone and ethanol three times.

2.3. Surface Functionalization of Silica Nanoparticles Using DAB Molecules. DAB molecules were immobilized onto the silica nanoparticle surface through the reaction of amine groups with carboxyl groups on the silica nanoparticles. The carboxyl groups were activated before the reaction. In the activation step, an aliquot was prepared by mixing together 2.5 mL of 100 mg/mL NHS, 2.5 mL of 100 mg/mL EDC, and 2.0 mL of 0.013 mg/mL carboxyl group modified nanoparticle solution. The mixture was allowed to react for 30 min. After the reaction, the products were washed with pH 7.4 buffer (PBS). Then, 100 μL of 2.14 mg/mL DAB solution was added. The mixture was stirred for 3 h, and the products were washed with the PBS buffer.

2.4. Determination of Selenium(IV) in Solution Using DAB Molecules. An aliquot of 0.10 mL of 0.05 M DAB solution (in 0.10 M HCl) was diluted to 5.0 mL using 0.10 M HCl. The DAB solution was heated in a 50.0 °C water bath for 5.0 min. Then, the Se(IV) solution was added to the DAB solution, which was left in the water bath for one hour. After 1.0 h of the reaction in the water bath, the pH of the solution was adjusted to 6−8 by adding HCl and NaOH solutions. Finally, an organic solvent, toluene, was added to the reaction solution. The DAB−Se complex was extracted to toluene from the aqueous solution. The fluorescence intensity of the DAB−Se complex in toluene was measured with a spectrofluorometer at 580 nm with an excitation wavelength of 420 nm.

2.5. Determination of Selenium in Real Samples Using SiNP−DAB Nanoprobes. Selenium(IV) in a real sample (cell culture solution, DMEM with 10% FBS) was determined using the developed nanoprobes. A 100 μL aliquot of DAB−NPs (1 mg/mL) was spiked with various concentrations of Se(IV) (final concentration, 8−64 ppm), and then the pH was adjusted to 4.5 using HCl and NaOH. The reaction procedure was the same as that of the Se determination using pure DAB. After the reaction, the pH of the mixture was adjusted to 6−8. To separate nanoparticles from the solution, the solution was filtered using a porous membrane with a pore size of 50 nm in diameter. The fluorescent nanoparticles were then dissolved in 2.5 mL of isopropanol−water mixture (1:1) for fluorescence measurements on the excitation wavelength of 420 nm.

2.6. Monitoring of Turn-on Fluorescence Signal Process under a Fluorescence Microscope. The fluorescence turn-on process was monitored under a fluorescence microscope. Glass slides were pretreated in a 10.0 M NaOH solution overnight, followed by thoroughly washing. The nanoprobes were mixed with selenium solution, and the mixture was placed on a glass slide after a certain period. After the samples were dried, the fluorescence images were taken using a 60× objective and a combination filter (exciter, XF1301, 415WB100; emitter, HQ535/50; splitter, Q505LP).

3. RESULTS AND DISCUSSION

3.1. Fabrication of the Nanoprobe. A wide variety of materials has been employed as matrices to fabricate various nanoprobes. Silica is one of the popular traditional materials used as a matrix for incorporating functional molecules.[33] The most attractive features of silica include nontoxicity,[34] high thermal stability, and effective transparency.[35] In recent years, nanoscale silica particles have been frequently used as a supporting matrix for making new nanomaterials, such as fluorescent tags, sensors, catalysts, etc.[29,36−43] Most importantly, the well established silica surface chemistry provides convenient pathways for immobilization of functional molecules onto the silica surface for probing target molecules. Thus, in this work, silica nanoparticles were chosen as a supporting matrix to make the selenium probe.

To make the turn-on fluorescent probe for selenium, the key step is to select a selenium-induced fluorescence molecule to turn

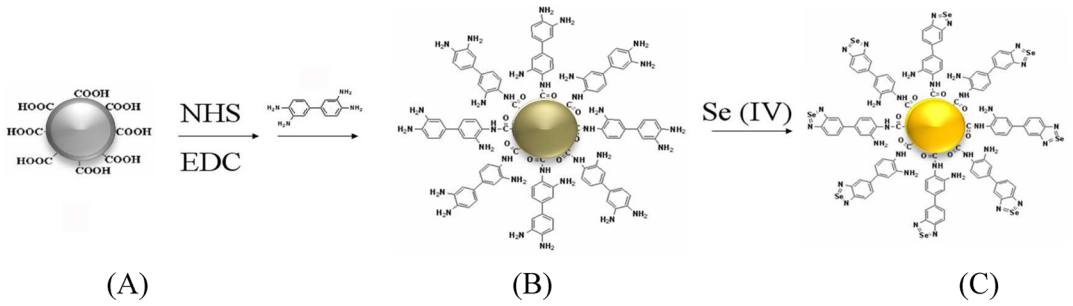

Figure 1. Schematic diagram of fabrication of the turn-on fluorescent nanoprobe for determination of selenium(IV). (A) Carboxyl group modified silica nanoparticle. (B) Nanoprobe for selenium. (C) The nanoprobe turned-on fluorescence signal when Se(IV) was present.

on the fluorescence signal when selenium is present. 3,3′-Diaminobenzidine (DAB) was previously used to signal selenium.[44] That study has proven that DAB can selectively react with selenium and produce a fluorescent complex of 3′,4′-diaminophenylpiazselenol.[44] Thus, in this work, DAB was chosen as a selenium probe molecule to make the nanoprobe.

After the matrix and probe molecules were selected, the immobilization of the probe molecules onto the silica nanoparticle surface is the essential step to make the nanoprobe. A DAB molecule has two pairs of amine groups on different sides, which makes immobilization of DAB to the nanoparticle surface possible. Based on the knowledge of chemical reactions, carboxyl groups can easily react with amine groups. Thus, bringing carboxyl groups onto the silica nanoparticle surface will be the next key step for fabrication of designed nanoprobes.

The carboxyl group modified silica nanoparticles have been developed in our previous work.[45] First a bare silica nanoparticle was synthesized using a reverse microemulsion method based on the polymerization of TEOS. Then, the silica nanoparticle was used as a core and the carboxyl groups were formed in an outer layer through a postcoating step. In this step, the polymerization of TOETAT was carried out, resulting in a COOH group layer on the silica nanoparticle surface.[45] The schematic diagram of the carboxyl-coated silica nanoparticle is shown in Figure 1A.

To initiate the reaction of carboxyl groups on the nanoparticle surface with amine groups on DAB molecules, the activation of carboxyl groups on the nanoparticles is necessary. 1-Ethyl-3-[3-dimethylaminopropyl] carbodiimide hydrochloride (EDC) was chosen for this activation since EDC can form *o*-acylisourea intermediates with the carboxyl groups on the surface of the nanoparticles. Afterward, *N*-hydroxysuccinimide (NHS) was applied to increase coupling efficiency of carboxyl groups with amine groups by forming active ester intermediates, which are more stable than *o*-acylisourea intermediates. Then DAB reacted with the intermediates and replaced the EDC and NHS. When the ratio of nanoparticles to DAB molecules was controlled properly, one amine pair group on a DAB molecule can link to the nanoparticle surface. Thus, the selenium nanoprobe was formed (Figure 1B). The other amine pair group on the DAB molecule can then bind to the target selenium and produce fluorescent complex (Figure 1C).

3.2. Characterization of the Nanoprobe. The morphology of the nanoprobes was characterized using a scanning electron microscope (SEM). First, the SEM images of the carboxyl group modified silica nanoparticles were taken. The results showed that the size of the silica nanoparticles was uniform (91 ± 6 nm in diameter, Figure 2A). The size of the silica nanoparticles is variable by changing the synthesis conditions.[33] After immobilization of DAB molecules on the nanoparticle, the size and shape of the nanoparticles have no significant changes (Figure 2B).

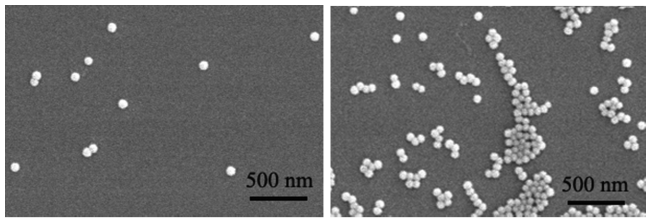

Figure 2. SEM images of carboxyl group- modified nanoparticles (A) and DAB functionalized nanoparticles (B).

To verify if the DAB molecules have been immobilized on the nanoparticle surface, UV−vis absorption spectrometry was employed to characterize the nanoprobes. The characterization was carried out from two angles. The first angle was to measure the amounts of DAB in solution both before and after it reacted with nanoparticles to investigate if the amount of DAB in the solution was decreased. A pure DAB aqueous solution was equally divided into two aliquots. One was used as a control whose absorption spectrum was obtained as shown in Figure 3A, curve a. Meanwhile, the other aliquot of DAB solution was used to react with silica nanoparticles. When the reaction was completed, the nanoparticles were filtered. The absorption spectrum of the DAB in the filtrate solution was obtained (Figure 3A, curve b). Compared to the control, curve a, the absorbance of DAB in the filtrate was obviously lower, indicating that some DAB molecules were immobilized onto the nanoparticles. According to the knowledge of chemical reaction, this was likely that the amine groups of DAB molecules had reacted with COOH groups on the silica nanoparticles.

To further verify this immobilization of DAB onto the nanoparticles, an additional experiment was carried out to measure the nanoparticles. Here, a pure silica nanoparticle solution was divided into two aliquots. One was used as a control, and the other was used to react with DAB molecules. After the reaction, the nanoparticles were filtrated and thoroughly washed. The absorption spectrum of pure silica nanoparticles is shown in Figure 3B, curve a. The absorption spectrum of DAB-reacted nanoparticles is shown in Figure 3B, curve b. To minimize the scattering from the silica nanoparticles, curve a was subtracted from curve b (inset in Figure 3B). In the differential spectrum, the DAB-reacted nanoparticles showed a clear absorption peak at about 320 nm and a shoulder at 290 nm, which were the featured absorption of DAB molecules. It appeared that the DAB molecules were successfully immobilized onto the silica

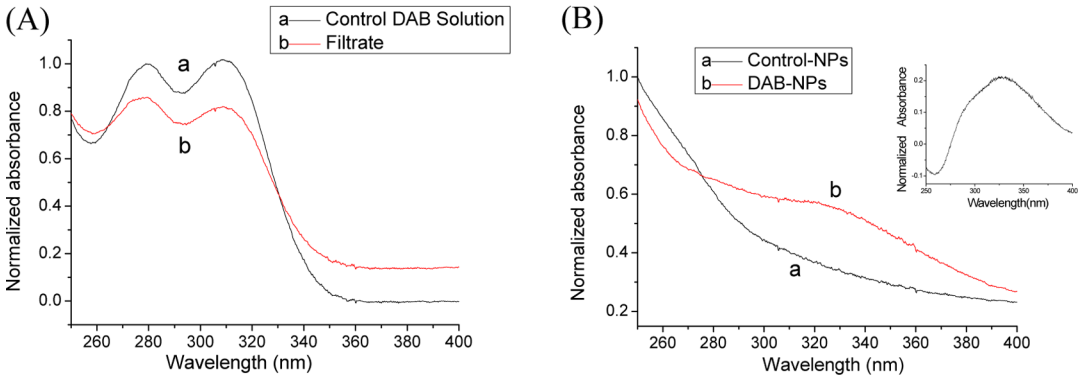

Figure 3. (A) UV−vis absorption spectra of DAB molecules in aqueous solution. (a) Pure DAB solution as a control. (b) After the DAB solution reacted with nanoparticles. (B) UV−vis absorption spectra of the nanoparticles. (a) Pure nanoparticle solution as a control (0.04 mg/mL). (b) Nanoparticle solution after reaction with DAB molecules. Inset: Curve a was subtracted from curve b.

nanoparticles, and thus a selenium nanoprobe was produced. There was a red-shift from about 20 nm. It could be caused by the formation of electron-withdrawing amide groups. The conjugation changed the symmetry of DAB's structure; this may contribute to the absorption change of immobilized DAB molecules. The number of DAB molecules on a single nanoprobe is controllable by changing the ratio of DAB molecules to silica nanoparticles.

3.3. In Situ Monitoring of Selenium-Induced Fluorescence Using the Turn-on Fluorescent Nanoprobe. The in situ monitoring of selenium(IV) using the developed nanoprobe was initially conducted in a selenium solution. As described in the Experimental Section, a fluorescence microscope was used to monitor the process of selenium-induced fluorescence. Before the nanoprobes reacted with the selenium solution, both a bright field image (Figure 4A1) and a fluorescence image (Figure 4A2) of the nanoprobes were taken. When these two images were combined, the merged image (Figure 4A3) clearly showed that the nanoprobes had no detectable fluorescence signals. As the nanoprobes started reacting with selenium, the fluorescence signal was turned on (Figure 4 B). As the reaction proceeded, more fluorescence signals appeared (Figures 4C−E). As the reaction time reached 2 h, all nanoprobes fluoresced (Figure 4F3). In this experiment, to clearly observe the in situ turn-on fluorescence of the nanoprobes, the selenium amount was in excess.

The increase of fluorescence signals from image Figure 4A to image Figure 4F indicated that more and more selenium(IV) were collected onto the nanoparticles, which meant that the nanoprobe was able to collect and enrich the target selenium onto the small domain of the nanoprobe. If this reaction was in solution, after the collection of target selenium, the nanoprobes could be separated from the solution by centrifuge. Thus, in addition to in situ monitoring of selenium, the nanoprobe could concentrate trace amount of target selenium. To verify the enriching target ability of the nanoprobe, a trace amount of selenium was reacted with the nanoprobe. After the reaction, the nanoprobes were collected and analyzed using an ICP-AES. The results showed that 0.077% (by weight, figure did not show) of selenium was presented in a single nanoprobe.

3.4. Determination of Selenium Using the Nanoprobes. The determination of selenium(IV) using DAB molecules has been studied previously.[6] These studies showed that several experimental conditions significantly affected fluorescence signals of the DAB−Se complex; in particular, solvent and pH considerably affected the fluorescence measurements. We repeated the literature method using DAB molecules. The results were similar to those reported in the literature. Since the nanoprobe provided a different environment for fluorescence measurement than the bulk solution, the optimization of experimental conditions was critical for application of the developed nanoprobe. The effects of solvent and pH were chosen as two major factors to study in this work. In addition, inferences of some common ions were studied.

Selection of an Optimal Solvent for the Nanoprobe. The fluorescence of the DAB−Se complex highly depended on the solvent polarity. The DAB−Se complex exhibited no fluorescence signal in pure water (Figure 5A, curve a). When the solvent was changed to a less polar organic compound, the DAB−Se complex could emit fluorescence. Toluene was commonly used as an effective solvent for the determination of Se(IV) with DAB. In toluene, DAB−Se showed a fluorescence emission peak at 580 nm with the excitation wavelength of 420 nm (Figure 5A, curve b). However, silica nanoparticles are hydrophilic. When the surface of the nanoparticles is not fully covered by DAB molecules, the solubility of the nanoprobes in toluene is problematic. Thus, it is necessary to select an effective organic solvent for the determination of selenium using the nanoprobe.

To choose an optimal solvent for this nanoprobe, three factors were considered as major criteria. In addition to the solvent harmfulness and fluorescence signal intensity of DAB−Se complex in the solvent, the amphiphilic property of the solvent is very important. A number of solvents were investigated for the nanoprobe based on these criteria. The results showed that isopropanol met the requirements well. The harmfulness of isopropanol is low; in fact it is lower than that of toluene. Meanwhile, isopropanol is partially amphiphilic, and DAB molecules have no fluorescence signals in isopropanol (Figure 5A, curve c), but DAB−Se complex fluoresces in isopropanol (Figure 5A, curve d). Compared to the fluorescence emission spectrum of DAB−Se complexes in toluene, a blue shift of the emission peak from 580 to 550 nm was observed in isopropanol. The nanoprobe−Se showed a greater blue shift to 530 nm in isopropanol (Figure 5 B). The blue shift is a common phenomenon of fluorophore aggregates. The phenomenon suggests a high density of the DAB molecules on the particle surface.[46]

In an isopropanol−water mixture, the fluorescence intensity of the DAB−Se complex depended on the ratio of the two solvents. If the volume ratio of isopropanol to water was 9:1, the 1×10^{-8} M complex exhibited intense fluorescence. With the same

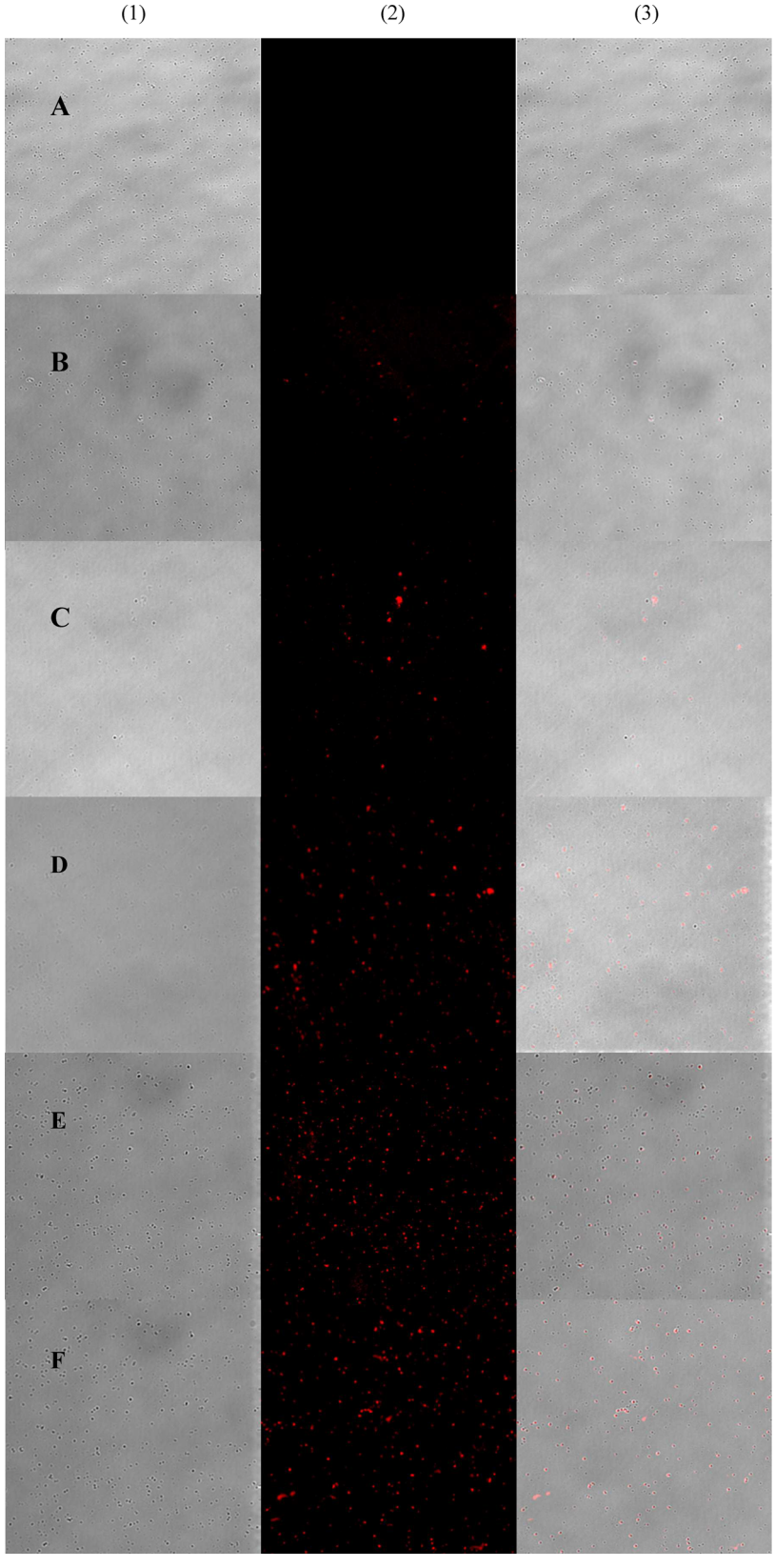

Figure 4. Monitoring of the fluorescence turned-on process when the nanoprobes interacted with selenium solution. Reaction time: (A) 0 min; (B) 15 min; (C) 30 min; (D) 60 min; (E) 90 min; (F) 120 min (F). (1) Bright field images, (2) fluorescence images, and (3) merged fluorescence and bright field images.

concentration, the intensity of the DAB−Se complex decreased dramatically as the decrease of the isopropanol percentage in the solution (Figure 6). This result suggested that the isopropanol percentage should be as high as possible. However, a high isopropanol percentage might cause the solubility problem of the DAB modified nanoprobe. Although isopropanol is partially

dx.doi.org/10.1021/am401015d | *ACS Appl. Mater. Interfaces* 2013, 5, 5165−5173

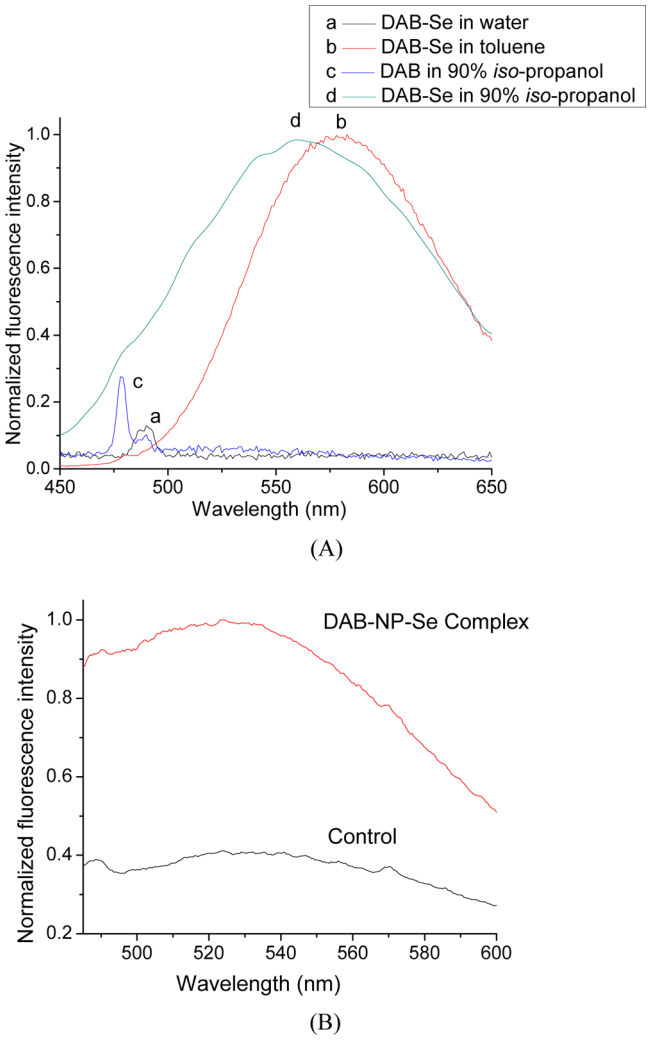

Figure 5. (A) Fluorescence emission of DAB−Se and DAB in various solvents. (a) DAB−Se in toluene, (b) DAB−Se in 90% isopropanol, (c) DAB−Se in water, (d) DAB in 90% isopropanol; (B) fluorescence emission of DAB−NP−Se in isopropanol.

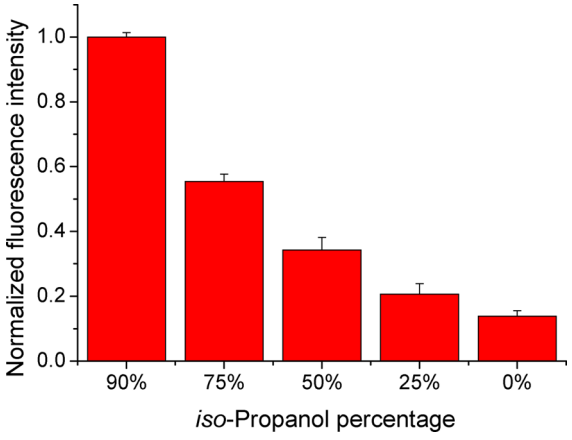

Figure 6. Fluorescence intensities of DAB−Se in mixtures of isopropanol with water.

amphiphilic, the solubility of the developed nanoprobes in isopropanol was not good enough. To further improve the solubility, a mixture of isopropanol and water was tested. The result showed that, if the isopropanol percentage is higher than 50%, the nanoprobes could be stably suspended in the isopropanol−water mixture. Thus, to balance the solubility of the nanoprobe and its fluorescence intensity, an optimal solvent mixture with the ratio of isopropanol to water of 1:1 was selected.

pH Effect. The fluorescence property of the DAB−Se complex is sensitive to the pH value of the solution. Acidic media give higher fluorescence signals. However, high acidity will lead to aggregation of the nanoprobes. Furthermore, the amide bonds between the nanoparticles and DAB will be broken at high acidity and thus damage the nanoprobe. Therefore, it is important to determine an optimal pH for the determination of selenium using the nanoprobe. A series of solution with various pH values was tested for the detection of selenium using the nanoprobe (Figure 7).

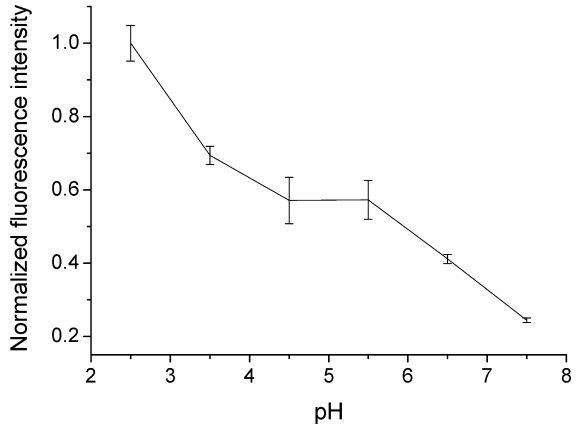

Figure 7. The solution pH effect on the fluorescence intensity of the nanoprobe−Se.

It was evident that the fluorescence intensity decreased as the pH increased. In the ranges of pH 2.5 to 3.5 and pH 5.5 to 7.5, the intensity changed dramatically. Meanwhile, obvious precipitation of the nanoprobes could be observed when the solution pH was lower than 4. However, in the range of pH 4.5 to 5.5, the fluorescence intensity remained constant. Thus, the pH range of 4.5 to 5.5 is suitable for determination of selenium using the nanoprobes. In this work, a value of pH 4.5 was used.

Selectivity of the Nanoprobe for Target Selenium. The selectivity of the developed nanoprobes for selenium was studied. The response of the nanoprobe to some common metal ions including Cu(II), Co(II), Zn(II), Pb(II), Mg(II), Hg(II), and Ca(II) was measured under the same experimental conditions. A concentration of 5.0 ppm was chosen for all common ions and selenium. The fluorescence signals of the nanoprobes to these common ions are shown in Figure 8. The fluorescence signal of the nanoprobe for selenium was 27 times higher than that of Hg(II), which gave the highest interference.

The exhibition of no or low fluorescence response from these metal ions only indicated that there was no positive interference from these ions for the determination of selenium. However, if negative interference existed to decrease fluorescence signals, the performance of the nanoprobe would be affected. Since the functional groups on the nanoprobe are amine groups, it is possible that metal ions can react with amines to occupy the Se(IV) binding sites, thus reducing the fluorescence signal. To test this possibility, an additional experiment was conducted in which common metal ions coexisted with selenium in the solution. The results showed that the majority of common metal ions had no negative interference for selenium determination.

dx.doi.org/10.1021/am401015d | ACS Appl. Mater. Interfaces 2013, 5, 5165−5173

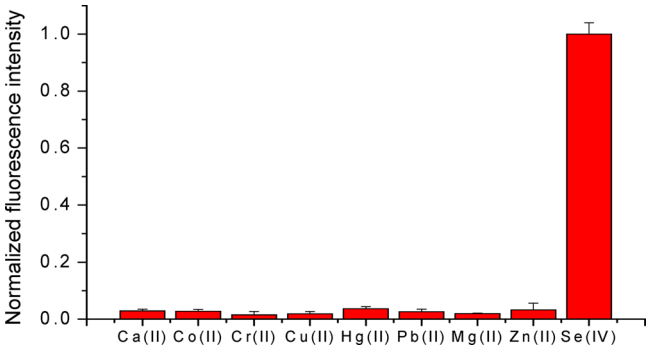

Figure 8. Comparison of the responses of the nanoprobe for common metal ions to the selenium ion.

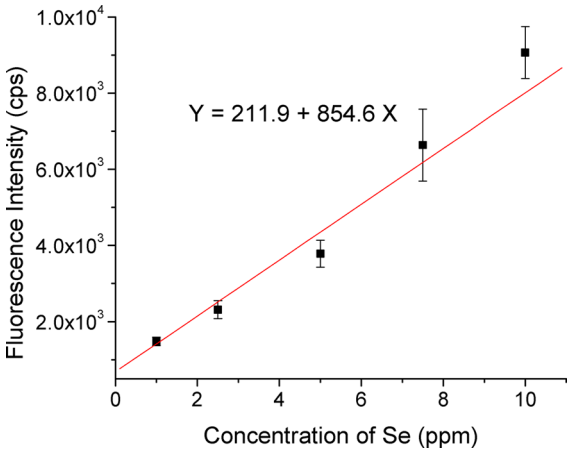

Figure 10. Linear range of the nanoprobe for determination of selenium(IV).

However, when Cu(II) coexisted with selenium, the fluorescence signal was significantly reduced by 62.4% (Figure 9A, from curve b to curve c). This result coincided with literature work.[44] To minimize the interference of Cu(II), ethylenediaminetetraacetic acid (EDTA) was used as a metal ion buffer. The coordination of EDTA with Cu(II) was strong enough to release the nanoprobe from Cu(II), resulting in an increase in fluorescence intensity (Figure 9A, curve d). The average results for Cu(II) interference and EDTA coordination effect are shown in Figure 9B. Therefore, if Cu(II) potentially exists in samples, EDTA coordination will be needed to reduce the interference.

Linear Range of the Nanoprobe for Determination of Selenium. The fluorescence emission at 530 nm with an excitation of 420 nm was chosen for the determination of selenium using the nanoprobe in a 50% isopropanol aqueous solution. The fluorescence intensity was proportional to the Se(IV) concentration. The linear range of this detection was 1.0−10.0 ppm (Figure 10) with a calibration equation of y = 211.9 + 854.6x. The detection limit was 0.19 ppm (2.41 μM). Both the linear range and the detection limit are not competitive to the most sensitive method of ICP-MS. However, the feature of in situ determination of selenium provides unique advantage of the developed nanoprobes. The application of this nanoprobe for in situ detection of selenium is in process.

Real Sample Detection. In certain practical samples, the concentration of other metal ions or some unknown contamination is significantly higher than that of Se(IV). Therefore, in addition to evaluating the DAB−SiNP probes in a lab water artificial system, we further investigated the performance of the nanoprobe in a real sample detection, i.e., cell culture solution (DMEM with 10% FBS). Figure 11 compared the response of this nanoprobe upon reaction with a blank cell culture solution and several cell culture samples spiked with various concentrations of Se(IV) (8−64 ppm). Importantly, this nanoprobe was inert toward the blank sample, which showed a very low fluorescence signal. The result suggested that the interference of other materials in the cell culture solution could not affect the detection. Moreover, there is a good linear relationship between the fluorescence intensity and the concentrations of Se(IV) (R^2 = 0.9913).

4. CONCLUSIONS

In summary, a novel turn-on fluorescence nanoprobe for determination of selenium was developed using silica nanoparticles as the matrix. The nanoprobe can selectively bind to selenium(IV) and emit fluorescence signals in situ. The fluorescence turn-on process was monitored using a fluorescence microscope. The ICP-AES method was used to identify the selenium that was collected by the nanoprobe. The fluorescence intensity of the nanoprobe is proportional to the selenium concentration. A solvent plays an important role for the measurement of the fluorescence signal. A mixture of a 1:1

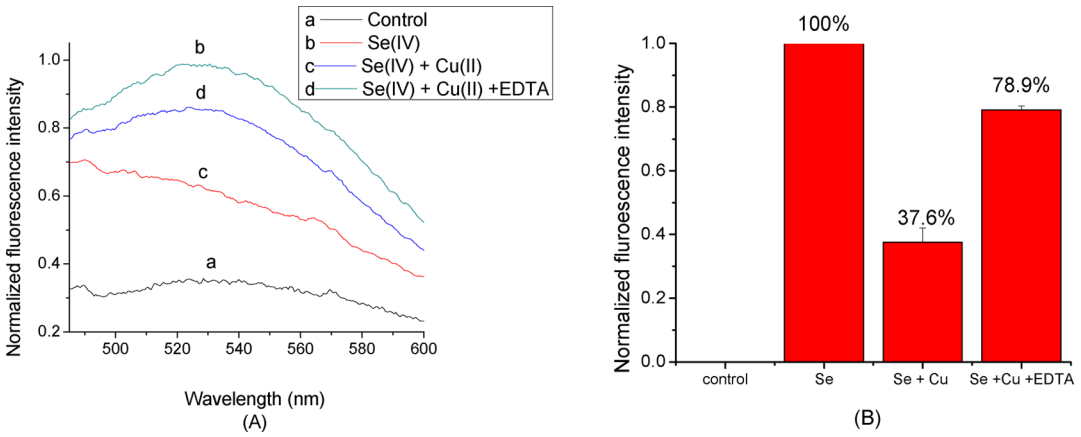

Figure 9. Interference of Cu(II) for the determination of selenium. (A) Fluorescence spectra: (a) blank signals, (b) pure selenium solution, (c) 5.0 ppm Cu(II) coexisting with selenium, and (d) EDTA + Cu(II) + Se(IV). (B) The influence of Cu(II) and the coordination effect of EDTA on the detected fluorescence signal by using the developed Se(IV) nanoprobes.

dx.doi.org/10.1021/am401015d | ACS Appl. Mater. Interfaces 2013, 5, 5165−5173

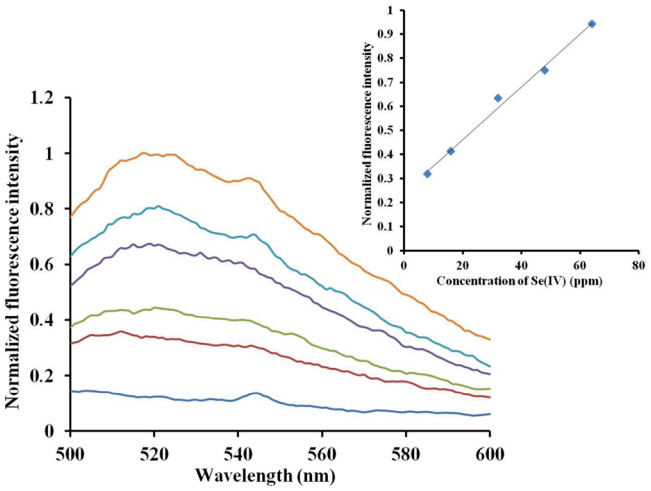

Figure 11. Fluorescence emission spectra of DAB−SiNPs in the presence of different concentrations of Se(IV). Excited at 420 nm with emission range from 500 to 600 nm. Slit: 2 nm. Inset: Linear fit of the fluorescence signal.

ratio of isopropanol to water can give an optimal fluorescence signal. The pH value significantly affects the detection. Considering the precision and stability of the nanoprobe in the process of the determination of selenium, pH 4.5−5.5 is a favorable range. With optimal conditions, the detection limit for selenium(IV) was 0.19 ppm (2.41 μM). The majority of common metal ions have no interference for the nanoprobe. Cu(II) can reduce the nanoprobe response to target, but EDTA could be used as an ion buffer to minimize the interference from Cu(II). Based on the optimum approach discovered in this study, a wide variety of desirable functionalized nanoprobes could be developed for enrichment and detection of various chemical and biological analytes. This study is expected to shed light on how to design turn-on fluorescent nanoprobes for in situ morning targets in biological processes.

AUTHOR INFORMATION

Corresponding Author

*E-mail: jzhao@chem.und.edu. Fax: 701-777-2331. Tel: 701-777-3610.

Notes

The authors declare no competing financial interest.

ACKNOWLEDGMENTS

This work was supported by the National Science Foundation under Grants CHE-0947043 and CHE-0911472. We thank Dr. Huawei Zeng in the USDA Grand Forks Human Nutrition Research Center for providing the cell culture solution for real sample detection. We also thank Ms. Jenny Sun at the Energy & Environmental Research Center for elemental analysis.

REFERENCES

(1) Zeng, H.; Davis, C. D.; Finley, J. W. *J. Nutr. Biochem.* **2003**, *14*, 227−231.
(2) Hill, K. E.; Xia, Y.; Akesson, B.; Boeglin, M. E.; Burk, R. F. *J. Nutr.* **1996**, *126*, 138−145.
(3) Carlson, B. A.; Novoselov, S. V.; Kumaraswamy, E.; Lee, B. J.; Anver, M. R.; Gladyshev, V. N.; Hatfield, D. L. *J. Biol. Chem.* **2004**, *9*, 8011−8017.
(4) López-Saez, J.-B; A. Senra-Varela, A.; Pousa-Estevez, L. *Oncology* **2003**, *64*, 227−231.
(5) Diwadkar-Navsariwala, V.; Prins, G. S.; Swanson, S. M.; Birch, L. A.; Ray, V. H.; Hedayat, S.; Lantvit, D. L.; Diamond, A. M. *Proc. Natl. Acad. Sci. U.S.A.* **2006**, *103*, 8179−8184.
(6) Dye, W. B.; Bretthauer, E.; Seim, H. J.; Blincoe, C. *Anal. Chem.* **1963**, *35*, 1687−1693.
(7) Bodini, M. E.; Pardo, J.; Arancibia, V. *Talanta* **1990**, *37*, 439−442.
(8) Chen, L.; Yang, F.; Xu, J.; Hu, Y.; Hu, Q.; Zhang, Y.; Pan, G. *J. Agric. Food Chem.* **2002**, *50*, 5128−5130.
(9) Bozsai, G.; Schlemmer, G.; Grobenski, Z. *Talanta* **1990**, *37*, 545−553.
(10) González-Nieto, J.; López-Sánchez, J. F.; Rubio, R. *Talanta* **2006**, *69*, 1118−1122.
(11) Machát, J.; Kanický, V.; Otruba, V. *Anal. Bioanal. Chem.* **2002**, *372*, 576−581.
(12) Masson, P.; Orignac, D.; Prunet, T. *Anal. Chim. Acta* **2005**, *545*, 79−84.
(13) Gómez-Ariza, J. L.; Pozas, J. A.; Giráldez, I.; Morales, E. *Talanta* **1999**, *49*, 285−292.
(14) Ishiyama, T.; Tanaka, T. *Anal. Chem.* **1996**, *68*, 3789−3792.
(15) Hazelton, S. G.; Pierce, D. T. *Anal. Chem.* **2007**, *79*, 4558−4563.
(16) Baraton, M., Ed. *Synthesis, Functionalization and Surface Treatment of Nanoparticles*; American Scientific Publisher.: Stevenson Ranch, CA, USA, 2003; pp 91−101.
(17) Edwards, R., Ed. *Immunoassays: Essential Data*; Wiley: New York, 1996; pp 63−75.
(18) Lakowicz, J. R. *Principles of Fluorescence Spectroscopy*; Springer: New York, 2006; pp 531−572.
(19) Alivisatos, A. P. *Science* **1996**, *271*, 933−937.
(20) Bruchez, M., Jr.; Moronne, M.; Gin, P.; Weiss, S.; Alivisatos, A. P. *Science* **1998**, *281*, 2013−2016.
(21) Pathak, S.; Choi, S.-K.; Arnheim, N.; Thompson, M. E. *J. Am. Chem. Soc.* **2001**, *123*, 4103−4104.
(22) Clark, H. A.; Kopelman, R.; Tjalkens, R.; Philbert, M. A. *Anal. Chem.* **1999**, *71*, 4837−4843.
(23) Xu, H.; Aylott, J. W.; Kopelman, R.; Miller, T. J.; Philbert, M. A. *Anal. Chem.* **2001**, *73*, 4124−4133.
(24) Zhao, Y.; Lin, Z.; He, C.; Wu, H.; Duan, C. *Inorg. Chem.* **2006**, *45*, 10013−10015.
(25) Ow, H.; Larson, D. R.; Srivastava, M.; Baird, B. A.; Webb, W. W.; Wiesner, U. *Nano Lett.* **2005**, *5*, 13−117.
(26) Santra, S.; Zhang, P.; Wang, K.; Tapec, R.; Tan, W. *Anal. Chem.* **2001**, *73*, 4988−4993.
(27) Xu, S.; Hartvickson, S.; Zhao, J. X. *Langmuir* **2008**, *24*, 7492−7499.
(28) Jin, Y.; Lohstreter, S.; Pierce, D. T.; Parisien, J.; Wu, M.; Hall, C.; Zhao, J. X. *Chem. Mater.* **2008**, *20*, 4411−4419.
(29) Zhao, X.; Tapec-Dytioco, R.; Tan, W. *J. Am. Chem. Soc.* **2003**, *125*, 11474−11475.
(30) Zhao, X.; Hilliard, L. R.; Mechery, S. J.; Wang, Y.; Bagwe, R. P.; Jin, S.; Tan, W. *Proc. Natl. Acad. Sci. U.S.A.* **2004**, *101*, 15027−15032.
(31) Wang, L.; Tan, W. *Nano Lett.* **2005**, *6*, 84−88.
(32) Chang, C.-L.; Fogler, H. S. *Langmuir* **1997**, *13*, 3295−3307.
(33) Wang, L.; Wang, K.; Santra, S.; Zhao, X.; Hilliard, L. R.; Smith, J. E.; Wu, Y.; Tan, W. *Anal. Chem.* **2006**, *78*, 646−654.
(34) Jin, Y.; Kannan, S.; Wu, M.; Zhao, J. X. *Chem. Res. Toxicol.* **2007**, *20*, 1126−1133.
(35) Cheben, P.; Monte, F. d.; Worsfold, D. J.; Carlsson, D. J.; Grover, C. P.; Mackenzie, J. D. *Nature* **2000**, *408*, 64.
(36) Sokolov, I.; Naik, S. *Small* **2008**, *4*, 934−939.
(37) Sokolov, I.; Kievsky, Y. Y.; Kaszpurenko, J. M. *Small* **2007**, *3*, 419−423.
(38) Santra, S.; Dutta, D.; A.Glenn, W.; Moudgil, B. M. *Technol. Cancer Res. Treat.* **2005**, *4*, 593.
(39) Zhao, X.; Bagwe, R. P.; Tan, W. *Adv. Mater.* **2004**, *16*, 173−176.
(40) Santra, S.; Wang, K.; Tapec, R.; Tan, W. *J. Biomed. Opt.* **2001**, *6*, 160−166.
(41) Santra, S.; Dutta, D.; A.Glenn, W.; Moudgil, B. M. *Technol. Cancer Res. Treat.* **2005**, *4*, 593−602.

(42) Clark, H. A.; Hoyer, M.; Philbert, M. A.; Hopelman, R. *Anal. Chem.* **1999**, *71*, 4831−4836.
(43) Loredana, L.; Amelia, M. *Langmuir* **2009**, *25*, 4767−4773.
(44) Cheng, K. L. *Anal. Chem.* **1956**, *28*, 1738−1742.
(45) Bagwe, R. P.; Hilliard, L. R.; Tan, W. *Langmuir* **2006**, *22*, 4357−4362.
(46) Yang, X.; Lu, R.; Zhou, H.; Xue, P.; Wang, F.; Chen, P.; Zhao, Y. *J. Colloid Interface Sci.* **2009**, *39*, 527−532.